Towards Rational Design of Fast Water-Exchanging Gd(dota-Like) Contrast Agents? Importance of the M/m Ratio**

Frank A. Dunand,[a] Rachel S. Dickins,[b] David Parker,[b] and André E. Merbach*[a]

Abstract: ^{1}H NMR line-shape analysis and magnetisation-transfer experiments at variable temperature and pressure have been used to elucidate the solution dynamics of both **M** and **m** isomers of three [Eu(dota-tetraamide)$(H_2O)]^{3+}$ complexes. The direct ^{1}H NMR observation of the bound water signal allows the water-exchange rates on each isomer to be measured individually. They are definitely independent of the ligand for both **M** and **m** isomers (**M**: $k_{ex}^{298} = 9.4 \pm 0.2 \times 10^3\ s^{-1}$ for $[Eu(dotam)(H_2O)]^{3+}$, $8.2 \pm 0.2 \times 10^3\ s^{-1}$ for $[Eu(dtma)(H_2O)]^{3+}$ and $11.2 \pm 1.4 \times 10^3\ s^{-1}$ for $[Eu(dotmam)(H_2O)]^{3+}$; **m**: $k_{ex}^{298} = 474 \pm 130 \times 10^3\ s^{-1}$ for $[Eu(dotam)(H_2O)]^{3+}$, $357 \pm 92 \times 10^3\ s^{-1}$ for $[Eu(dtma)(H_2O)]^{3+}$), and proceed through a dissociative mechanism (**M** isomers: $\Delta V^{\ddagger} = +4.9\ cm^3\ mol^{-1}$ for $[Eu(dotam)(H_2O)]^{3+}$ and $+6.9\ cm^3\ mol^{-1}$ for $[Eu(dtma)(H_2O)]^{3+}$). The overall water exchange only depends on the **M**/**m** isomeric ratio. The **m** isomer, which exchanges more quickly, is favoured by α-substitution of the ring nitrogen. Therefore the synthesis of DOTA-like ligands, which predominantly form complexes in the **m** form, should be a sufficient condition to ensure faster water exchange on potential Gd^{III}-based contrast agents. Furthermore the activation parameters for the water-exchange and isomerisation processes are both compatible with a nonhydrated complex as intermediate.

Keywords: contrast agents · lanthanides · ligand design · magnetic resonance imaging · solution dynamics · water exchange

Introduction

Since the introduction of Gd complexes as MRI contrast agents, there has been an intense research effort to understand their physico-chemical properties.[1–3] One of the important points to be understood in order to design new Gd^{III}-based MRI contrast agents is the relationship between the complex structure and the rate and mechanism of the water-exchange process as this is one of the limiting factors, along with the tumbling time and the electronic relaxation rate.[4, 5] Our interest here embraces the solution dynamics of [Ln(dota-like)(H_2O)] complexes (DOTA = 1,4,7,10-tetraaza-1,4,7,10-tetrakis(carboxymethyl)cyclododecane). These compounds exist in two diastereomeric forms, **M** and **m**: The **M** isomer has a square antiprismatic geometry, while the **m** isomer has a twisted square antiprismatic arrangement of the ligand.[6] Basically, the two structures display a different orientation of the two square planes formed by the four nitrogens and the four oxygens; they make an angle of about 40° in **M**-type structures, whereas this angle is reversed and reduced to about 28° in the **m**-type derivatives. Such arrangements appear common to all chelates containing DOTA-like ligands. Unfortunately when one analyses the ^{17}O transverse relaxation rates of the free water by the Swift and Connick method, it is very hard to obtain information about the individual exchange rates.

Eu^{III}, the neighbour of Gd^{III}, is often used, as structural NMR is possible on its equivalent complexes. Recently, the bound water signal could be observed by NMR at low temperature in a mixture of water and CD_3CN on the positively charged Eu^{III} complex of DOTAM, the tetraamide derivative of DOTA, as a consequence of a very slow water-exchange rate (DOTAM = 1,4,7,10-tetrakis(carbamoylmeth-

[a] Prof. A. E. Merbach, F. A. Dunand
Institut de Chimie Minérale et Analytique, Université de Lausanne, 1015 Lausanne (Switzerland)
Fax: (+41) 21-692-38-75
E-mail: andre.merbach@icma.unil.ch

[b] Dr. R. S. Dickins, Prof. D. Parker
Department of Chemistry, University of Durham
South Road, Durham, DH1 3LE (UK)

[**] High-Pressure NMR Kinetics, Part 96; for Part 95 see: L. Burai, E. Tóth, S. Seibig, R. Scopelliti, A. E. Merbach, *Chem. Eur. J.* **2000**, *6*, 3761 – 3370.

Supporting Information for this article is available on the WWW under http://wiley-vch.de/home/chemistry/ or from the author. Example of the 4-site exchange analysis; temperature and pressure dependence of the bound water-proton line widths of $[Eu(dtma)(H_2O)]^{3+}$; temperature and dependence of the bound water-proton line widths of $[Eu(dotmam)(H_2O)]^{3+}$; Two-dimensional EXSY ^{1}H NMR spectra of $[Eu(dtma)(H_2O)]^{3+}$ and $[Eu(dotmam)(H_2O)]^{3+}$; temperature dependence of the **M**/**m** equilibrium constant as well as M_{ax1} and m_{eq2} proton line widths of the *RRRS*/*SSSR* isomer of $[Eu(dotmam)(H_2O)]^{3+}$; pressure dependence of the M_{ax1} line widths isomer of $[Eu(dotmam)(H_2O)]^{3+}$; pressure dependence of the **M**/**m** equilibrium constant of the *RRRR*/*SSSS* and *RRRS*/*SSSR* isomers of $[Eu(dotmam)(H_2O)]^{3+}$; volume profiles for the **M**/**m** systems; thermodynamic, kinetic and activation parameters describing the *RRRS*/*SSSR*, *RSRS* and *RRSS* isomers of $[Eu(dotmam)(H_2O)]^{3+}$; experimental data for the temperature and pressure dependence of the line widths, interconversion rates and equilibrium constants of $Eu(dtma)(H_2O)]^{3+}$ and $[Eu(dotmam)(H_2O)]^{3+}$.

  0947-6539/01/0723-5160 $ 17.50+.50/0

yl)-1,4,7,10-tetraazacyclododecane).[7] This allowed the unambiguous determination of the individual water-exchange rates on each isomer. The rate was 50 times faster on the **m** species, which therefore contributes 80% of the observed water-exchange rate.[8, 9]

Lately, the influence of the different water-exchange rates of the two isomers has been detected on slowly exchanging bis- or tetraamide DOTA-derivative Gd^{III} complexes from the temperature dependence of the ^{17}O transverse relaxation rates of the free water.[10, 11] Important errors are probably related to this indirect determination of the exchange rates as many processes are involved in the ^{17}O transverse relaxation rates. Nevertheless Woods et al., neglecting the contribution of the **M** isomer, found the same water-exchange rate for the **m** isomers of $[Gd(dota)(H_2O)]^-$, $[Gd(dotma)(H_2O)]^-$ and three isomers of an α-substituted DOTA-derivative complex (DOTMA = 1,4,7,10-tetrakis(methylcarboxymethyl)-1,4,7,10-tetraazacyclododecane). They thus proposed a direct correlation between the isomeric composition and the observed water-exchange rate.[11]

Our goal is here to directly and independently measure the water exchange for each isomer in a series of three tetraamide DOTA-derivative Eu^{III} complexes (Figure 1), and hence determine unambiguously the role of the **M**/**m** isomeric ratio. We also intend to extend our understanding of the correlation between water exchange and $\mathbf{M} \rightleftharpoons \mathbf{m}$ interconversion[9] by solving the solution dynamics on the basis of diverse variable-temperature and -pressure ^1H NMR experiments.

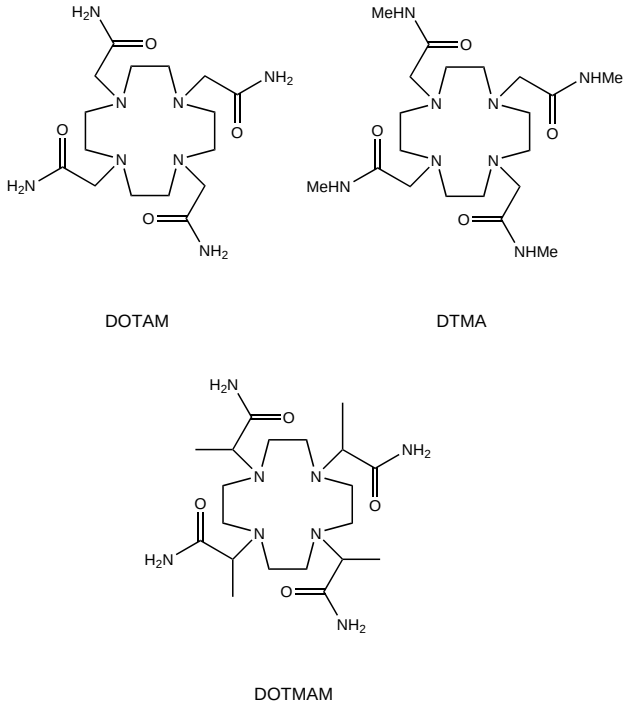

Figure 1. Schematic representation of the three studied ligands.

Results

Structural aspect: The ^1H NMR spectra of $[Eu(dotam)(H_2O)]^{3+}$ and $[Eu(dtma)(H_2O)]^{3+}$ (DTMA = 1,4,7,10-tetrakis(*N*-methylcarbamoylmethyl)-1,4,7,10-tetraazacyclododecane) have already been published and are typical for complexes possessing a C_4 axis of symmetry for both **M** and **m** isomers.[8] A second small series of signals, visible in the case of $[Eu(dtma)(H_2O)]^{3+}$, is probably due to a minor species with a different binding geometry of the proton and methyl substituents in the methylamide unit (<4%). In the $[Eu(dotmam)(H_2O)]^{3+}$ complex (DOTMAM = 1,4,7,10-tetrakis(methylcarbamoylmethyl)-1,4,7,10-tetraazacyclododecane), the substitution on the α-C of the amide arm produces a new chiral centre. The stereogenicity at carbon is the source of the four isomers observed in solution (see Figures 2 and 3):

i) the four centres have the same absolute configuration (*RRRR*/*SSSS*), the complex retains its C_4 symmetry, and only one signal is observed for each proton of the ligand (4);
ii) the *R* and *S* configurations alternate around the ligand (*RSRS*), hence the complex has a C_2 symmetry and two signals are observed (3,10);
iii) one centre differs from the others (*RRRS*/*SSSR*), the complex has a C_1 symmetry and four signals are observed (1,5,6,9);
iv) two *R* centres alternate with two *S* centres, the complex has a C_1 symmetry and four signals are observed (2,7,8,11).

The attribution of the *RRRR*/*SSSS* and *RSRS* isomers is obvious. The *RRRS*/*SSSR* and *RRSS* isomers were attributed on the basis of related analyses[11, 12] in which α-substituted complexes were diastereospecifically synthesised.

Water exchange: The slow water exchange allows the observation of the bound water signal by ^1H NMR of the $[Eu(dtma)(H_2O)]^{3+}$ and $[Eu(dotmam)(H_2O)]^{3+}$ complexes, as

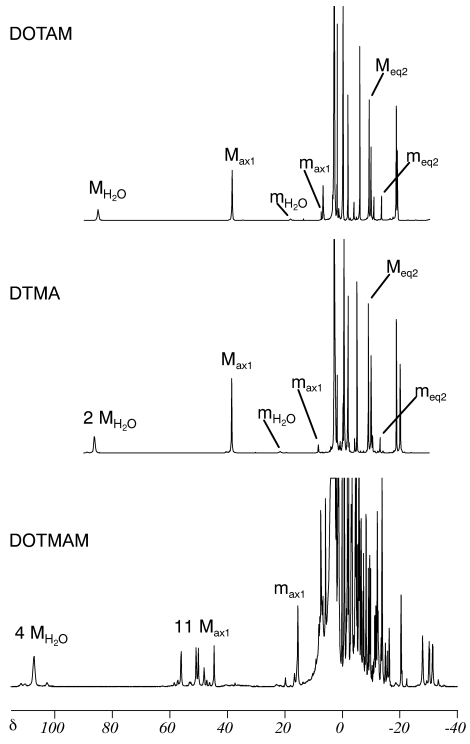

Figure 2. ^1H spectra of the $[Eu(dotam)(H_2O)]^{3+}$ (219 K), $[Eu(dtma)(H_2O)]^{3+}$ (220 K) and $[Eu(dotmam)(H_2O)]^{3+}$ (219 K) complexes (**M** or **m** isomers) depicting the bound water signals and the ligands signals used for the analysis (CD_3CN/H_2O 100:1, 9.4 T).

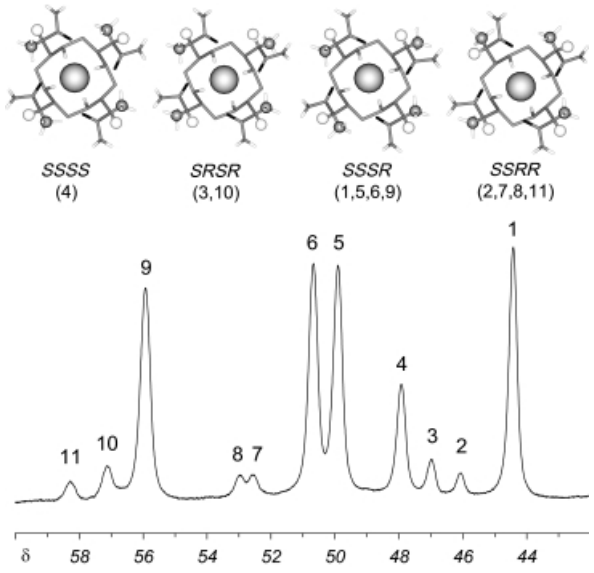

Figure 3. ^{1}H NMR spectrum of the $[Eu(dotmam)(H_2O)]^{3+}$ complex (CD_3CN/H_2O 100:1, 9.4 T, 219 K) showing the attribution of the **M** axial resonances: *RRRR*/*SSSS* = 4; *RSRS* = 3,10; *RRSS* = 2,7,8,11; *SRRR*/*RSSS* = 1,5,6,9.

was the case for $[Eu(dotam)(H_2O)]^{3+}$.[7–9] In the case of $[Eu(dtma)(H_2O)]^{3+}$, the signal is detected for both **M** and **m** isomers, and two signals are even visible for the **M** isomer (vide supra). For the $[Eu(dotmam)(H_2O)]^{3+}$ complex, four **M** signals arise, one for each of the four isomers described above, while no **m** signals could be detected (see Figure 2). We have previously demonstrated by ^{17}O NMR that the exchange phenomenon observed on the bound water proton corresponds to the exchange of the entire water molecule.[9] Hence, we can use the temperature dependence of the ^{1}H NMR bound water signals to determine the water-exchange rates and their activation parameters.

At the temperatures at which the bound water signals are observable, the slow exchange approximation [Eq. (1)] applies.

$$\pi W_{1/2}^{B} = \frac{1}{T_{2B}^{meas}} = \frac{1}{T_{2B}} + \frac{1}{\tau_B} \quad (1)$$

$W_{1/2}^{B}$ is the measured half width of the bound water signal, $1/T_{2B}$ is the transverse relaxation rate in the absence of exchange and τ_B is the residence time of the water molecule in the first coordination sphere. The temperature dependence of the water-exchange rate k_{ex} ($= 1/\tau_B$) can be described by the Eyring equation [Eq. (2)], in which the symbols have their usual meaning.

$$\frac{1}{\tau_B} = k_{ex} = k_{ex}^{298}\frac{T}{298.15}\exp\left[\frac{\Delta H^{\ddagger}}{R}\left(\frac{1000}{298.15} - \frac{1000}{T}\right)\right] \quad (2)$$

$1/T_{2B}$ is assumed to follow an exponential Arrhenius law [Eq. (3)] incorporating different contributions (dipolar and contact for proton).

$$\frac{1}{T_{2B}} = \left(\frac{1}{T_{2B}}\right)^{298.15}\exp\left[\frac{E_a}{R}\left(\frac{1000}{T} - \frac{1000}{298.15}\right)\right] \quad (3)$$

The bound water line widths have been fitted to Equations (1) – (3) (Figure 4) to yield the kinetic parameters

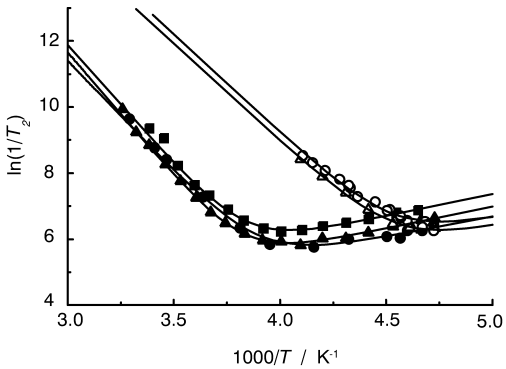

Figure 4. Temperature dependence of the bound water proton transverse relaxation rates of the **M** and **m** isomers of the $[Eu(dotam)(H_2O)]^{3+}$ (●: **M**, ○: **m**), $[Eu(dtma)(H_2O)]^{3+}$ (▲: **M**, △: **m**) and $[Eu(dotmam)(H_2O)]^{3+}$ (■: **M**) complexes (CD_3CN/H_2O 100:1, 9.4 T).

reported in Table 1 and partly in the Supporting Information (Table S20). For the **M** isomer of $[Eu(dtma)(H_2O)]^{3+}$ or $[Eu(dotmam)(H_2O)]^{3+}$, the analysis was performed with the main signal only, but the smaller signal(s) show the same temperature dependence (see Supporting Information Figures S2 and S4).

At a given temperature, the water-exchange rate depends on pressure following Equation (4), in which $\Delta V^{\ddagger}$ is the activation volume of the water-exchange reaction and $k_{ex,0}$ is the exchange rate at zero pressure.

$$k_{ex} = k_{ex,0}\exp\left(\frac{-\Delta V^{\ddagger}}{RT}P\right) \quad (4)$$

The measured line width is related to k_{ex} by Equation (1). The effect of pressure on the transverse relaxation rate in the absence of exchange ($1/T_{2B}$) can be neglected: first because

Table 1. Kinetic and activation parameters describing the water exchange as determined by line-shape analysis of the ^{1}H NMR bound water signals of the **M** and **m** isomers of the $[Eu(dotam)(H_2O)]^{3+}$, $[Eu(dtma)(H_2O)]^{3+}$ and $[Eu(dotmam)(H_2O)]^{3+}$ complexes.

	$[Eu(dotam)(H_2O)]^{3+}$[a]		$[Eu(dtma)(H_2O)]^{3+}$		$[Eu(dotmam)(H_2O)]^{3+}$	
	M	**m**	**M**	**m**	**M**	**m**
k^{250} [10^3 s^{-1}]	0.090 ± 0.008	10.2 ± 1	0.066 ± 0.005	7.9 ± 0.6	0.111 ± 0.015	–
k^{298} [10^3 s^{-1}]	9.4 ± 0.2	474 ± 130	8.2 ± 0.2	357 ± 92	11.2 ± 1.4	–
$\Delta H^{\ddagger}$ [kJ mol^{-1}]	57.5 ± 1	47.2 ± 3	59.7 ± 1	46.7 ± 3	57.2 ± 3	–
$\Delta S^{\ddagger}$ [J K^{-1} mol^{-1}]	+ 24.1 ± 4	+ 22 ± 11	+ 30.3 ± 4	+ 18.0 ± 10	+ 24.4 ± 10	–
$\Delta V^{\ddagger}$ [cm^3 mol^{-1}]	+ 4.9 ± 1	–	+ 6.9 ± 0.5	–	–	–

[a] In order to allow comparison of the results, we report here for $[Eu(dotam)(H_2O)]^{3+}$ the values obtained by the fit of the ^{1}H NMR data only in ref. [25].

0947-6539/01/0723-5162 $ 17.50+.50/0 *Chem. Eur. J.* **2001**, *7*, No. 23

the overall contribution of $1/T_{2B}$, calculated from the parameters obtained in the variable temperature study [Eq. (3)], is less than 10% for the ^{1}H NMR measurements at 285 K; second because the pressure dependence of $1/T_{2B}$ itself is known to be small.[13]

In the case of $[Eu(dtma)(H_2O)]^{3+}$, the line width of the bound water signal of the **M** isomer was measured at different pressures from 0.1 to 200 MPa. The evolution of $\ln(1/T_2^{meas})$ of the proton signal upon changes in pressure is shown in the Supporting Information (Figure S3). The activation volume calculated from the ^{1}H NMR data is $\Delta V^{\ddagger} = 6.9 \pm 0.5\ cm^3 mol^{-1}$.

$\mathbf{M} \rightleftharpoons \mathbf{m}$ interconversion:

Generalities and theory: Two sources of helicity are present in $[Eu(dota\text{-}like)(H_2O)]^{3+}$ complexes.[14] One is due to the four 5-membered rings formed by the binding of the amide arms to Eu^{III}, whose absolute configuration is described by Δ or Λ. The second is due to the four 5-membered rings formed by the binding of the cyclen to Eu^{III}, its absolute configuration is described by $\delta\delta\delta\delta$ and $\lambda\lambda\lambda\lambda$. Hence two different processes can lead to an $\mathbf{M} \rightleftharpoons \mathbf{m}$ interconversion: i) a rotation of the amide arms around the N(cycle)–C bond leading to a Δ-Λ configurational change; ii) an inversion of the cyclen cycle configuration ($\delta\delta\delta\delta$-$\lambda\lambda\lambda\lambda$). The enantiomerisation most probably proceeds by successive occurrence of these two processes. Scheme 1 summarises these concepts in a visual manner.

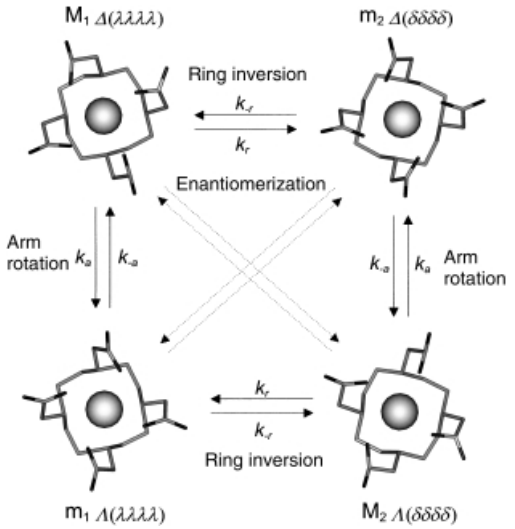

Scheme 1. Schematic representation of the four possible conformational isomers of DOTA-derivative complexes and their interconversion pathways. The protons as well as the coordinated water molecule located above the plane of the four carboxylates have been omitted for clarity.

The ^{1}H NMR ligand resonances for $[Eu(dotam)(H_2O)]^{3+}$ and $[Eu(dtma)(H_2O)]^{3+}$ have already been attributed in previous papers.[7, 8] From Scheme 1 it is clear that the arm rotation does not affect the geometry of the cyclen unit, and hence a ring axial proton remains axial upon arm rotation. On the other hand, the ring inversion moves a proton from an axial position into an equatorial position (and vice versa). Consequently the four resonances depicted by M_{ax1}, m_{ax1}, M_{eq2} and m_{eq2} in Figure 2 form a closed 4-site exchange system.

Two-dimensional-EXSY ^{1}H NMR experiments were performed at 284 K with a mixing time of 100 ms on both $[Eu(dtma)(H_2O)]^{3+}$ and $[Eu(dotmam)(H_2O)]^{3+}$ complexes. In the case of $[Eu(dtma)(H_2O)]^{3+}$, cross-peaks corresponding to arm rotation, ring inversion and enantiomerisation are visible, while for $[Eu(dotmam)(H_2O)]^{3+}$ only ring inversion is detected (See Supporting Information Figure S5). Moreover the signals that are part of the same M_{ax1}, m_{ax1}, M_{eq2} and m_{eq2} system were identified from these experiments.

This exchange behaviour was further confirmed by magnetisation-transfer experiments on $[Eu(dtma)(H_2O)]^{3+}$ (261 K) and $[Eu(dotmam)(H_2O)]^{3+}$ (273 K). All magnetisation-transfer experiments were performed by using an I-Burp shaped pulse for the selective inversion of the M_{ax1} signal. For $[Eu(dotmam)(H_2O)]^{3+}$, the analysis was performed on the two main *RRRR*/*SSSS* and *RRRS*/*SSSR* isomers.

When one process is favoured over the others, like ring inversion in the case of $[Eu(dotmam)(H_2O)]^{3+}$, the intensities of the two signals involved (M_{ax1} and m_{eq2}) can be fitted to the McConnell equations.[15, 16] When two processes are in concurrence, we are in a 4-site exchange case.

The time dependency of the magnetisation in a magnetisation-transfer experiment in which *i* sites are involved can be described by modified Bloch equations[17] in which the chemical exchange is taken into account.[18]

$$\frac{dM_{zi}}{dt} - \omega_i v_i = \frac{-M_{zi}}{\tau_{1i}} + \sum_{j=1}^{n} k_{ji} M_{zj} + \frac{M_i^{\infty}}{T_{1i}} \qquad (5)$$

where:

$$\frac{1}{\tau_{1i}} = \frac{1}{\tau_i} + \frac{1}{T_{1i}}$$

$$\frac{1}{\tau_i} = \sum_{j \neq 1} k_{ij}$$

Since the relaxation times are measured in the absence of the rf (radio frequency) field, the term $\omega_i v_i$ can be neglected ($\omega_i = \gamma H_i$ and v_i is the component of the spin magnetisation out of phase with the rf field). M_i^{∞} is the equilibrium magnetisation and T_{1i} is the longitudinal relaxation time of the i^{th} site.

If one considers that the enantiomerisation is only possible through successive arm rotation and ring inversion, the differential equations describing the time evolution of the magnetisation only depend on two first-order rates and two populations as depicted in Scheme 1; where k_a is the rate of the arm rotation leading from the **M** to the **m** isomer, k_r is the rate of the ring inversion leading from the **M** to the **m** isomer and p_M and p_m are the populations of the **M** and **m** isomers, respectively. On this basis the rate of the arm rotation leading from **m** to **M** can be written as $(p_M/p_m)k_a$. The magnetisation-transfer experiment following the selective inversion of the M_1 site is described by the following set of differential equations:

$$\frac{dM_1}{dt} = \frac{M_1^{\infty} - M_1}{T_{1M_1}} - k_a M_1 - k_r M_1 + \frac{p_M}{p_m} k_a m_1 + \frac{p_M}{p_m} k_r m_2 \qquad (6)$$

$$\frac{dm_1}{dt} = \frac{m_1^{\infty} - m_1}{T_{1m_1}} + k_a M_1 + k_r M_2 - \frac{p_M}{p_m} k_a m_1 - \frac{p_M}{p_m} k_r m_1 \qquad (7)$$

$$\frac{dm_2}{dt} = \frac{m_2^{\infty} - m_2}{T_{1m_2}} + k_r M_1 + k_a M_2 - \frac{p_M}{p_m} k_a m_2 - \frac{p_M}{p_m} k_r m_2 \quad (8)$$

$$\frac{dM_2}{dt} = \frac{M_2^{\infty} - M_2}{T_{1M_2}} - k_a M_2 - k_r M_2 + \frac{p_M}{p_m} k_a m_2 + \frac{p_M}{p_m} k_r m_1 \quad (9)$$

An example of the analysis of such a system is shown in the Supporting Information (Figure S1).

Quantitative analysis: *[Eu(dtma)(H$_2$O)]$^{3+}$*: As we have just pointed out, both arm-rotation and ring-inversion exchanges are observed and, hence, they both contribute significantly to the line-broadening upon temperature changes. A simple line-shape analysis would not give information about the kinetic and activation parameters of the individual processes. Therefore magnetisation-transfer experiments were performed at various temperatures between 261 and 282 K. They were analysed with the differential Equations (6) to (9) to provide k_a, k_{-a}, k_r and k_{-r} at each temperature. The temperature dependence of the M_{ax1} and m_{ax1} line widths were then measured. These experiments were both performed in a 1:1 mixture of CD_3CN and D_2O in order to avoid the presence of nonhydrated complexes in solution. The line width of a ligand proton belonging to the **M** species can be described by simply modifying Equation (1) [Eq. (10)], in which $1/T_{2B}$ contains the dipolar and contact contribution to the transverse relaxation rate, and k_a and k_r are the two possible exchange contributions (k_{-a}, k_{-r} in the case of **m**).

$$\pi W_{1/2}^{B} = \frac{1}{T_2^{meas}} = \frac{1}{T_{2B}} + k_a + k_r \quad (10)$$

k_a and k_r follow an Eyring [Eq. (2)] and $1/T_{2B}$ an exponential Arrhenius [Eq. (3)] dependence with temperature. The rates and the line widths were then fitted simultaneously to Equations (2), (3) and (10) to afford the parameter values reported in Table 2 (and partially in the Supporting Information Table S21). The goodness of this analysis is clearly depicted in Figure 5.

In the same way, the pressure dependence of the rates and line widths were fitted simultaneously (Figure 6) by using Equations (4) and (10). As explained for the water exchange, the pressure dependence of $1/T_{2B}$ was assumed to be negligible (contribution to the line width is less than 20% with only a small variation with pressure).

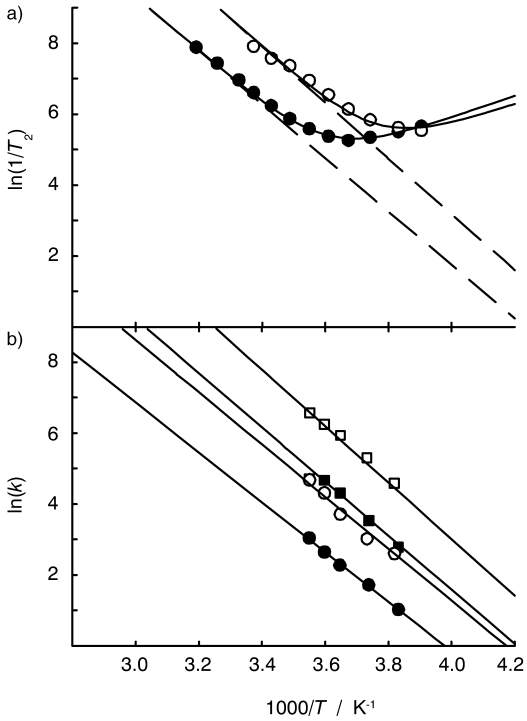

Figure 5. a) Temperature dependence of the ^{1}H NMR transverse relaxation rates of the M_{ax1} (●) and m_{ax1} (○) of the [Eu(dtma)(H$_2$O)]$^{3+}$ complex (CD_3CN/D_2O 1:1, 9.4 T). b) Temperature dependence of the **M** → **m** arm rotation (■), ring inversion (●) and **m** → **M** arm rotation (□), ring inversion (○) rates of the [Eu(dtma)(H$_2$O)]$^{3+}$ complex as obtained by magnetisation transfer on the M_{ax1} and m_{ax1} signal (CD_3CN/D_2O 1:1, 9.4 T). The solid lines represent the best simultaneous fit to all experimental data points in the Figure, and the dotted lines represent the exchange contribution to the line widths (see text and Table 2).

Quantitative analysis: *[Eu(dotmam)(H$_2$O)]$^{3+}$*: We have shown that the exchange contribution to the line width is exclusively due to the ring inversion process (vide supra). Thus the line-shape analysis will give direct information about the kinetic and activation parameters that describe the ring inversion. As for [Eu(dtma)(H$_2$O)]$^{3+}$, these experiments were performed in a 1:1 mixture of CD_3CN and D_2O in order to avoid the presence of nonhydrated complexes in solution. The equilibrium constant $K = \mathbf{M}/\mathbf{m}$ (measured directly from the integrals) was also taken into account in the analysis as it can be

Table 2. Kinetic, activation and thermodynamic parameters describing the solution behaviour of the three studied complexes. The fitting method for each case is explained in details in the text.

	[Eu(dotam)(H$_2$O)]$^{3+}$ Arm rotation		[Eu(dtma)(H$_2$O)]$^{3+}$ Arm rotation		[Eu(dtma)(H$_2$O)]$^{3+}$ Ring inversion		[Eu(dotmam)(H$_2$O)]$^{3+}$[a] Ring inversion	
	M → **m**	**m** → **M**	**M** → **m**	**m** → **M**	**M** → **m**	**m** → **M**	**M** → **m**	**m** → **M**
k^{250} [10^3 s^{-1}]	68 ± 10	310 ± 10	4.4 ± 0.3	27.7 ± 4	0.9 ± 0.1	3.1 ± 0.3	1.8 ± 0.5	0.4 ± 0.1
k^{298} [10^3 s^{-1}]	1700 ± 200	7650 ± 200	671 ± 43	3192 ± 330	79.5 ± 5	430 ± 53	232.9 ± 25	70.7 ± 8
$\Delta H^{\ddagger}$ [kJ mol^{-1}]	39.1 ± 2	39.1 ± 2	62.5 ± 2	58.8 ± 3	55.9 ± 1	61.0 ± 3	60.2 ± 3	63.9 ± 3
$\Delta S^{\ddagger}$ [J K^{-1} mol^{-1}]	− 52.1 ± 7	− 39.4 ± 7	+ 18.7 ± 6	+ 19.4 ± 10	− 21.1 ± 5	+ 10.1 ± 10	+ 2.3 ± 11	+ 4.8 ± 11
$\Delta V^{\ddagger}$ [cm^3 mol^{-1}]	− 0.5 ± 0.3	− 0.5 ± 0.7	+ 0.7 ± 2	–	+ 3.3 ± 0.9	–	+ 1.6 ± 2	− 1.1 ± 0.6
K^{250}	4.5[b]		4.2 ± 0				0.23 ± 0.01	
K^{298}	4.5[b]		5.2 ± 2				0.30 ± 0.01	
ΔH^0 [kJ mol^{-1}]	–[b]		2.8 ± 3				3.7 ± 1	
ΔS^0 [J K^{-1} mol^{-1}]	–[b]		+ 23.2 ± 10				2.6 ± 3	
ΔV^0 [cm^3 mol^{-1}]	0 ± 1		− 2.6 ± 2				− 1.7 ± 6	

[a] *RRRR/SSSS* isomer. [b] Undetectable variation, hence no thermodynamic parameters given.

0947-6539/01/0723-5164 $ 17.50+.50/0 *Chem. Eur. J.* **2001**, *7*, No. 23

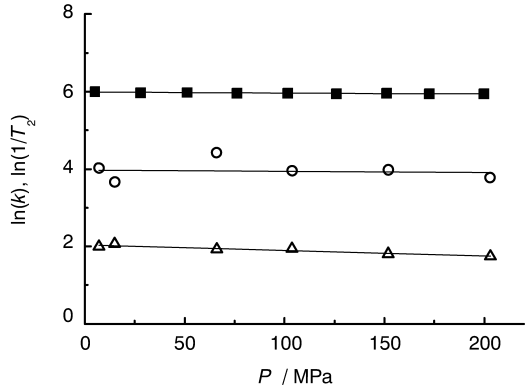

Figure 6. Pressure dependence of the ^{1}H NMR transverse relaxation rates of the M_{ax1} signal at 284 K (■); as well as of the arm rotation (○) and ring inversion (△) rates at 271 K as obtained by magnetisation transfer for the $[Eu(dtma)(H_2O)]^{3+}$ complex (CD_3CN/D_2O 1:1, 9.4 T). The lines represent the best simultaneous fit to all experimental data points in the Figure (see text and Table 2).

expressed directly from the rate constants $K = k_{-r}/k_r$. The ring-inversion rate measured by magnetisation transfer at 273 K was introduced into the analysis to constrain the exchange rate beyond the exchange domain. We show in Figure 7 the temperature dependence of the line widths and equilibrium constant as well as the ring-inversion rate obtained by magnetisation transfer for the *RRRR*/*SSSS* isomer. The parameters obtained from their analysis are reported in Table 2 (and partially in the Supporting Information Table S22). The analysis of the pressure dependence was performed separately for transverse relaxation rates and the equilibrium constant (see Supporting Information Figures S7 and S8). The fit of the *RRRS*/*SSSR* system is also shown in the Supporting Information (Figure S6), as well as all parameters describing the solution behaviour of the *RRRS*/*SSSR*, *RRSS* and *RSRS* isomers (Tables S17–S19, S23).

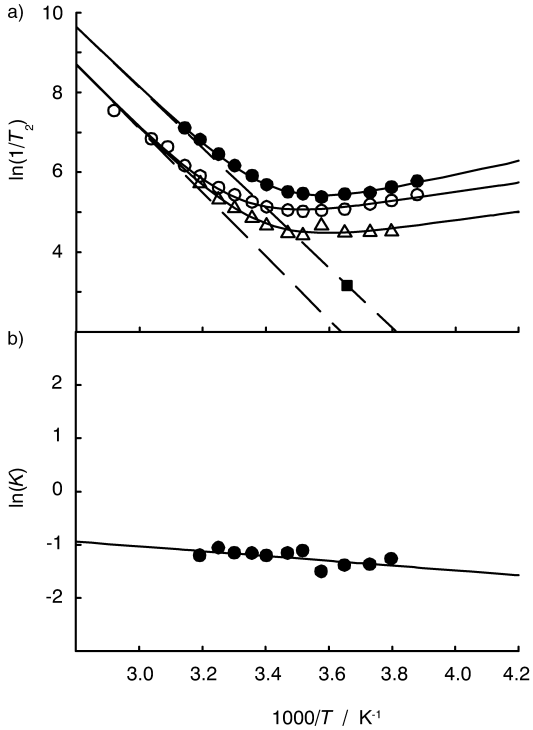

Figure 7. a) Temperature dependence of the ^{1}H NMR transverse relaxation rates of the M_{ax1} (●), m_{ax1} (○) and m_{eq2} (△) signals and ring inversion rate measured by magnetisation transfer (■) of the *RRRR*/*SSSS* isomer of the $[Eu(dotmam)(H_2O)]^{3+}$ complex (CD_3CN/D_2O 1:1, 9.4 T). b) Temperature dependence of the equilibrium constant $K = \mathbf{M}/\mathbf{m}$ (●). The solid lines represent the best simultaneous fit to all experimental data points in the Figure and the dotted lines represent the exchange contribution to the line widths (see text and Table 2).

Discussion

Water exchange: Recently Woods et al.[11] indirectly estimated the exchange rate of the **m** isomers of a series of pure diastereomers of Gd^{III} tetra(carboxyethyl)dota complexes on the basis of the temperature dependence of the ^{17}O NMR transverse relaxation rate of the free water. They assumed the contribution of the **M** isomer to be negligible and, from the overall exchange rate and the molar fraction of the **m** isomer, found the same exchange rate on **m** for all species.

Here, we could directly and individually determine the water-exchange rates of the individual isomers of a series of $[Eu(dota\text{-}tetraamide)(H_2O)]^{3+}$ complexes. From the kinetic parameters reported in Table 1, as well as from Figure 4, it is obvious that the water exchange of both **M** and **m** isomers is independent of the ligand, it is even the same for all isomers of $[Eu(dotmam)(H_2O)]^{3+}$ (See Supporting Information, Figure S4). Therefore, if we extend this behaviour to gadolinium we can conclude that the overall water-exchange rate on Gd(dota-like) complexes is only determined by the ratio of the **M** and **m** isomers. This is an important feature in our desire to better understand how to rationally design new contrast agents with enhanced relaxivity.

M ⇌ m interconversion: Previous studies of $[Ln(dota)(H_2O)]^-$ complexes with ^{1}H two-dimensional EXSY[19, 20] or variable-temperature ^{13}C NMR[6, 21] showed that the arm rotation is faster than the ring inversion. The introduction of a substituent at the α position of the ring nitrogen drastically slows down the arm rotation, so that ring inversion becomes the faster process.[12]

The series of ligand studied here clearly shows the influence of the substituent on the rate of the interconversion processes. The arm rotation is slowed down in the case of DTMA but remains the fastest process. α-Substitution however imparts such steric hindrance on the arm rotation process that it can no longer be detected. The ring inversion rate remains of the same order of magnitude for each complex (see Table 2). We reanalysed the magnetisation-transfer experiment on the DOTAM complex at 250 K with the four-site system, the rate of k_r ($1.0 \pm 0.6\ s^{-1}$) is the same as for DTMA.

Furthermore, the equilibrium constant $K = \mathbf{M}/\mathbf{m}$ is confirmed to be linked to the rigidity brought by the steric hindrance due to the substitution on the arm. In particular, the α-substituted *RRRR*/*SSSS* isomers tends to stabilise the **m** form of the complex; the introduction of a bulky amide also seems to follow this tendency.[8, 11, 12]

Solution dynamics: The thermodynamic and activation parameters allow us to visually represent the solution dynamics by free energy (Figure 8) and volume (Supporting Information, Figure S9) profiles. In fact, the parameters obtained for

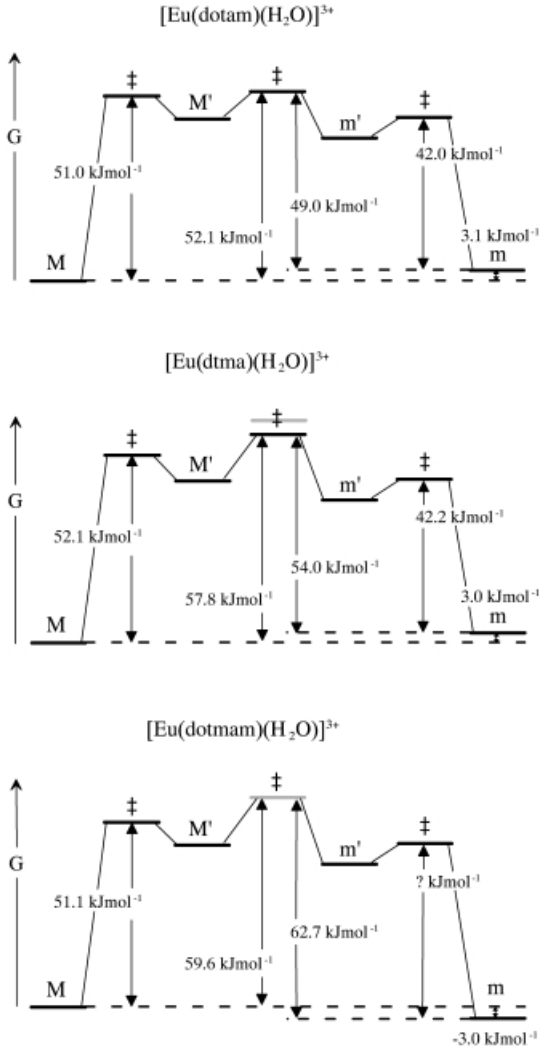

Figure 8. Free-energy profiles for the **M**/**m** systems, considering nonhydrated eight-coordinated intermediates **M**′ and **m**′ in both the water-exchange and the interconversion processes. In the case of the interconversion transition state: black level = arm rotation; grey level = ring inversion. The levels of the *RRRR*/*SSSS* species are considered for the $[Eu(dotmam)(H_2O)]^{3+}$ complex.

DTMA and DOTMAM extend the validity of the model proposed for DOTAM[9] considering nonhydrated eight-coordinated intermediates **M**′ and **m**′ in both the water-exchange and isomerisation processes. Two experimental observations confirm this trend: i) the activation volume of the water exchange of $[Eu(dtma)(H_2O)]^{3+}$ is clearly positive ($\Delta V^{\ddagger} = 6.9 \pm 0.5\ cm^3\,mol^{-1}$); this shows the mechanism to be dissociative; ii) the observation of an exchange (broadening of the ligand signals corresponding to the water-exchange rate) with a nonhydrated species in solution in the presence of a very low quantity of water (Supporting Information, Figure S10).

Conclusion

^1H NMR line-shape analysis and magnetisation-transfer experiments at variable temperature and pressure have been used to elucidate the solution dynamics of [Eu(dota-tetraamide)$(H_2O)]^{3+}$ complexes. The water-exchange rate is definitely independent of the solution structure for both **M** and **m** isomers, and, hence, the overall water exchange only depends on the **M**/**m** isomeric ratio. The faster exchanging **m** isomer is favoured by α-substitution of the ring N. Therefore, the synthesis of DOTA-like ligands that predominantly form complexes in the **m** form should be a sufficient condition to ensure fast water exchange for potential Gd^{III}-based contrast agents.

Experimental Section

Ligands and complex synthesis: The DTMA and DOTAM ligands and their complexes were prepared as previously described.[7, 8, 22]

1,4,7,10-tetrakis(methylcarbamoylmethyl)-1,4,7,10-tetraazacyclododecane (DOTMAM): A slurry of 1,4,7,10-tetraazacyclododecane (200 mg, 1.16 mmol) and potassium carbonate (880 mg, 5.8 mmol) in dry DMF (5 mL) was added to a solution of 2-bromopropionamide (880 mg, 5.8 mmol) in dry DMF (5 mL). The solution was heated for 24 h, the solvent removed under reduced pressure, and the resultant residue was partitioned between water (10 mL) and dichloromethane (10 mL). The aqueous layer was separated, washed with dichloromethane (2×10 mL), evaporated and taken up into dry methanol (10 mL). The methanol was filtered, the solvent was removed under reduced pressure, and the residue taken up in methanol again. This process was repeated three times. The resultant residue was recrystallised from water to yield a colourless solid. Yield: 260mg, 50 %; ^1H NMR (300 MHz, D_2O, TMS): $\delta = 3.37$ (br m, 4H; CH), 2.63 – 2.54 (br m, 16H; ring CH_2), 1.05, (br dd, 12H; Me); MS (ESI): *m*/*z* (%): 457 (100) $[MH]^+$, 248 (20) $[MCa^{2+}]$; elemental analysis calcd (%) for $[C_{20}H_{40}N_8O_4.H_2O]$: C 49.58, H 8.67, N 23.1; found C 49.75, H 8.88, N 23.0.

$[Eu(dotmam)(H_2O)](CF_3SO_3)_3$: This was prepared as described for the corresponding DTMA complex. MS (ESI): *m*/*z* (%) 202.7 (100) $[EuL^{3+}]$, 304.5 (30) $[EuL^{2+}]$, 379.4 (10) $[EuLCF_3SO_3^{2+}]$; elemental analysis calcd (%) for $[C_{23}H_{40}EuF_9N_8O_{10}S_3]$: C 27.41, H 4.06, N 11.11; found C 27.66, H 4.17, N 10.95.

Sample preparation: The solutions for NMR analysis were prepared by dissolution of the solid complex $[Eu(L)(H_2O)](SO_3CF_3)_3$ in CD_3CN and H_2O or D_2O with a drop of TMS as an internal reference. The Eu^{III} concentration varied from 5 to 20 mM, and the water content was 1 % for the solutions containing H_2O and 50 % for the solutions containing D_2O.

Variable temperature NMR: The ^1H NMR spectra were measured on a Bruker DPX-400 spectrometer. The temperature was stabilised by a Bruker BVT-3000 temperature control unit, and checked by a substitution method.[23]

Variable Pressure NMR: The ^1H NMR measurements were performed by using a narrow-bore 5 mm home-built ^1H-specific high-pressure probe head on a ARX-400 Bruker spectrometer.[24] The pressure was produced by a manual pump, and $C_2Br_2F_4$ was used as pressurisation liquid. The temperature was stabilised by using industrial alcohol in a Huber cryothermostat HS80 and checked with a Pt probe (Pt-100 Ω) connected to a calibrated digital Data Tracker 130 (Data Oricess Instrument, USA).

Data treatment: The NMR signals were fitted by a lorentzian function with the program NMRICMA 2.8 for MATLAB® (L. Helm, A. Borel, Institut de Chimie Minérale et Analytique, Université de Lausanne, Switzerland). The half-width of the ^1H NMR lines were corrected by subtracting the half-width of the TMS line (inhomogeneity, line broadening). The integrals were calculated by multiplying the fitted half-width by the height of the lines. The simultaneous fitting of the data (line width and/or magnetisation transfer) to obtain the kinetic and thermodynamic parameters was

0947-6539/01/0723-5166 $ 17.50+.50/0 *Chem. Eur. J.* **2001**, *7*, No. 23

performed by the programs VISUALISEUR 2.2.4 and OPTIMISEUR 2.2.4 for MATLAB® (F. Yerly, 1999, Institut de Chimie Minérale et Analytique, Université de Lausanne, Switzerland).

Acknowledgement

This work was financially supported by the Swiss National Research Foundation (FNRS) and the Swiss OFES as part of the EU COST D18 Action "Lanthanide Chemistry for Diagnosis and Therapy".

[1] *The Chemistry of Contrast Agents in Medical Magnetic Resonance Imaging* (Eds.: A. E. Merbach, E. Tóth), Wiley, New York, **2001**.
[2] P. Caravan, J. J. Ellison, T. J. McMurry, R. B. Lauffer, *Chem. Rev.* **1999**, *99*, 2293 – 2352.
[3] R. B. Lauffer, *Chem. Rev.* **1987**, *87*, 901 – 927.
[4] E. Tóth, L. Helm, A. E. Merbach in *The Chemistry of Contrast Agents in Medical Magnetic Resonance Imaging* (Eds.: A. E. Merbach and E. Tóth), Wiley, New York, **2001**, Chapter 2.
[5] D. H. Powell, O. M. Ni Dhubhghaill, D. Pubanz, Y. Lebedev, W. Schlaepfer, A. E. Merbach, *J. Am. Chem. Soc.* **1996**, *118*, 9333 – 9346.
[6] S. Aime, M. Botta, G. Ermondi, *Inorg. Chem.* **1992**, *31*, 4291 – 4299.
[7] S. Aime, A. Barge, M. Botta, A. S. De Sousa, D. Parker, *Angew. Chem.* **1998**, *110*, 2819 – 2820; *Angew. Chem. Int. Ed.* **1998**, *37*, 2673 – 2675.
[8] S. Aime, A. Barge, J. I. Bruce, M. Botta, J. A. K. Howard, J. M. Moloney, D. Parker, A. S. De Sousa, M. Woods, *J. Am. Chem. Soc.* **1999**, *121*, 5762 – 5771.
[9] F. A. Dunand, S. Aime, A. E. Merbach, *J. Am. Chem. Soc.* **2000**, *122*, 1506 – 1512.
[10] S. Zhang, Z. Kovacs, S. Burgess, S. Aime, E. Terreno, A. D. Sherry, *Chem. Eur. J.* **2001**, *7*, 288 – 296.
[11] M. Woods, S. Aime, M. Botta, J. A. K. Howard, J. M. Moloney, M. Navet, D. Parker, M. Port, O. Rousseaux, *J. Am. Chem. Soc.* **2000**, *122*, 9781 – 9792.
[12] J. A. K. Howard, A. M. Kenwright, J. M. Moloney, D. Parker, M. Port, M. Navet, O. Rousseau, M. Woods, *Chem. Commun.* **1998**, 1381 – 1382.
[13] K. Micskei, L. Helm, E. Brücher, A. E. Merbach, *Inorg. Chem.* **1993**, *32* (*18*), 3844 – 3850.
[14] S. Aime, M. Botta, M. Fasano, M. P. M. Marques, C. F. G. C. Geraldes, D. Pubanz, A. E. Merbach, *Inorg. Chem.* **1997**, *36*, 2059 – 2068.
[15] H. M. McConnell, *J. Chem. Phys.* **1958**, *28*, 430 – 431.
[16] J. J. Led, H. Gesmar, *J. Magn. Res.* **1982**, *49*, 444 – 463.
[17] F. Bloch, *Phys. Rev.* **1946**, *70*, 460 – 474.
[18] J. Schotland, J. S. Leigh, *J. Magn. Res.* **1983**, *51*, 48 – 55.
[19] S. Hoeft, K. Roth, *Chem. Ber.* **1993**, *126*, 869 – 873.
[20] V. Jacques, J. F. Desreux, *Inorg. Chem.* **1994**, *33*, 4048 – 4053.
[21] S. Aime, A. Barge, M. Botta, M. Fasano, J. D. Ayala, G. Bombieri, *Inorg. Chim. Acta* **1996**, *246*, 423 – 429.
[22] S. Amin, J. R. Morrow, C. H. Lake, M. R. Churchill, *Angew. Chem.* **1994**, *106*, 824 – 826; *Angew. Chem. Int. Ed. Engl.* **1994**, *33*, 773 – 775.
[23] C. Ammann, P. Meier, A. E. Merbach, *J. Magn. Res.* **1982**, *46*, 319 – 321.
[24] A. Cusanelli, L. Nicula-Dadci, U. Frey, A. E. Merbach, *Inorg. Chem.* **1997**, *36*, 2211 – 2217.
[25] S. Aime, A. Barge, M. Botta, L. Frullano, U. Merlo, K. I. Hardcastle, *J. Chem. Soc. Dalton Trans.* **2000**, 3435 – 3440.

Received: June 7, 2001 [F3319]